JCTC Journal of Chemical Theory and Computation

ARTICLE

pubs.acs.org/JCTC

Evaluating the Performance of DFT Functionals in Assessing the Interaction Energy and Ground-State Charge Transfer of Donor/Acceptor Complexes: Tetrathiafulvalene−Tetracyanoquinodimethane (TTF−TCNQ) as a Model Case

Gjergji Sini,[†] John S. Sears, and Jean-Luc Brédas*

School of Chemistry and Biochemistry and Center for Organic Photonics and Electronics, Georgia Institute of Technology, Atlanta, Georgia 30332-0400, United States

ABSTRACT: We have evaluated the performance of several density functional theory (DFT) functionals for the description of the ground-state electronic structure and charge transfer in donor/acceptor complexes. The tetrathiafulvalene−tetracyanoquinodimethane (TTF−TCNQ) complex has been considered as a model test case. Hybrid functionals have been chosen together with recently proposed long-range corrected functionals (ωB97X, ωB97X-D, LRC-ωPBEh, and LC-ωPBE) in order to assess the sensitivity of the results to the treatment and magnitude of exact exchange. The results show an approximately linear dependence of the ground-state charge transfer with the $HOMO_{TTF}-LUMO_{TCNQ}$ energy gap, which in turn depends linearly on the percentage of exact exchange in the functional. The reliability of ground-state charge transfer values calculated in the framework of a monodeterminantal DFT approach was also examined.

INTRODUCTION

Since the initial works by Mulliken et al.,[1] donor−acceptor (charge-transfer) complexes have long been of interest. Recently, they have attracted increased attention due to their role in organic opto-electronic devices and in particular in organic solar cells[2] and organic light-emitting diodes.[3] The performance of organic photovoltaic devices primarily depends on the electronic structure at the interface between an electron donor (D) component and an acceptor (A) component in both the ground and excited states. In the excited state, the ability of an exciton present either on the donor or on the acceptor to dissociate into a charge-transfer (D^+/A^-) state determines the extent of the generated photocurrent; in the ground state, the nature of the electronic interactions between donor and acceptor directly impacts the charge recombination ($D^+/A^- \rightarrow D/A$) process[4] as well as the reverse electrical current in the dark.[5] In organic light-emitting diodes, ground-state charge transfer between a charge-transport molecule and a molecular dopant that form a D/A complex is observed in a number of instances to greatly facilitate charge injection from an electrode into the charge-transport material.[3,6] We focus here on the ground state of D/A complexes (while the description of the electronic structure in the lowest charge-transfer excited state will be addressed in a forthcoming work).

We are particularly interested in assessing the reliability of DFT methodologies to evaluate the interaction energy between the D and A molecules and the amount of charge transfer in the ground electronic state. DFT methods have been largely used for the study of such issues[7] but intrinsically lead to a stabilization of the virtual molecular orbitals (MOs) with respect to the occupied MOs.[8] This is due to (i) the fact that the virtual orbital energies in DFT are defined with respect to an N-electron problem vs $N+1$ in Hartree−Fock (HF) theory and (ii) the self-interaction error[9] that induces, for example, spurious long-range stabilization upon dissociation,[10] overestimates charge-transfer properties,[11] and results in substantial errors for long-range charge-transfer excitations.[12] The inclusion of some amount of exact HF exchange within the exchange functional is one approach often used to remedy these problems;[13] however, such "hybrid" functionals have been found to fail for the description of long-range interactions. Other methods[14] make use of the error function (erf) in order to separate the (r^{-1}) Coulomb operator into a short-range and a long-range region, using for example hybrid meta-GGA functionals for the description of the short-range interactions (the first term on the rhs of eq 1) and HF exchange for the long-range interactions (second term):

$$\frac{1}{r_{12}} = \frac{1-\mathrm{erf}(\omega r_{12})}{r_{12}} + \frac{\mathrm{erf}(\omega r_{12})}{r_{12}} \qquad (1)$$

The use of such functionals, referred to as ω functionals, has led in general to important improvements, specifically in the description of charge-transfer (CT) excited states.[15] The ω parameter in eq 1 defines the extent of the short- and long-range regions and is typically taken as a constant optimized for a given functional. However, it has been demonstrated that the delineation between short- and long-range components (optimal ω) is a function of the electronic density of the system under study.[16] In order to take this effect into account, Stein et al.[15] recently proposed a simple method for optimizing the ω value for each particular system, leading to much better results, for example, in the case of CT excited-state calculations.

In the limit of the complete transfer of one electron from donor to acceptor, the ground-state wave function becomes that of an open-shell singlet and, as a result, is not well described by

Received: September 24, 2010
Published: January 18, 2011

single-reference methods. The reliability of the ground-state charge-transfer values computed within the confines of DFT has been examined previously.[17] Geskin et al.[17b] have underlined that, in the limit of weak coupling (vanishing wave function overlap) between donor and acceptor, integer charge-transfer values should be expected; i.e., the charge transfer should be either near zero or near unity. This points consequently to the necessity of a multiconfigurational description. Although spin-unrestricted DFT approaches may provide a qualitatively correct description of the charge transfer in such cases,[17b] this almost certainly results in a spin-polarized description of the electronic wave function. When considering single-reference HF and spin-restricted DFT approaches for weakly coupled complexes, the ground-state charge transfer was shown to vary in a continuous manner as a function of the (donor) HOMO−(acceptor) LUMO energy gap, while the charge-transfer values computed with multireference methods provided the expected 0-to-1 stepwise evolution.[17b]

The same description applies in the intermediate coupling regime, as shown by Avilov et al.[17a] in the case of a tetrathiafulvalene−tetracyanoquinodimethane (TTF−TCNQ) complex. However, these authors pointed out that, in instances where the charge-transfer values are small (lower than ∼0.2*e*), the CASSCF and monodeterminantal RHF calculations actually give similar partial charge-transfer values, with a gradual increase in the amount of charge transferred as the $HOMO_{TTF}-LUMO_{TCNQ}$ energy gap decreases. As for the strong coupling regime, single molecule electron transport measurements[18] and calculations[19] have shown that the amount of charge transferred is expected to vary continuously with the voltage between electrodes. Thus, the applicability of single-reference methods for describing D/A charge transfer depends upon the strength of the electronic coupling; in addition, when single-reference DFT methods are indeed applicable, the reliability of the charge-transfer values computed with DFT methods depends as well on the choice of the functional.

The aim of our study is to analyze the performance of various DFT functionals for the description of the charge transfer in the ground state of donor−acceptor complexes. As a test case, we have chosen the TTF−TCNQ complex, as it represents a D/A complex that has been largely studied previously and for which partial charge transfer is expected; TCNQ derivatives are also widely used as molecular dopants in organic light-emitting diodes.[3] The DFT functionals were chosen to include hybrid functionals with a low percentage of HF exchange (B3LYP,[13,20] TPSSh,[21] B97-1,[22] B97-2,[23] and PBE0[24]), hybrid functionals with a high percentage of HF exchange (BMK,[25] BHandH,[26] BHandHLYP,[27] M05-2X,[28] M06−2X,[29] M06-HF[29]), and some of the more recent ω functionals (ωB97X[30] and ωB97X-D,[31] as well as LRC-ωPBEh[32] and LC-ωPBE[33]).

THEORETICAL METHODS

Computations were performed with the Gaussian 09,[34] QChem 3.2,[35] and Molpro 2009[36] packages. The isolated monomers of TTF and TCNQ were completely optimized (RMS gradient 10^{-3}) at the M05-2X/6-311G** level of theory. Geometries for the TTF−TCNQ complex were constructed in cofacial and parallel-displaced configurations (employing the frozen-monomer approximation) by varying the distance between the molecular centers along the *z* axis and (in the case of the parallel-displaced configurations) the *y* axis, see Figure 1. A fixed *z* distance (3.45 Å) between the molecular planes was chosen for the parallel-displaced configurations. Single-point computations were performed at the level of second-order Møller−Plesset perturbation theory (MP2),[37] spin-component-scaled (SCS)-MP2,[38] and DFT levels of theory employing a 6-311++G** basis and various functionals as described above. All of the functionals have been applied as defined in the literature and implemented in their respective programs, with the exception of ωB97X. For the ωB97X functional, results are presented for two ω values: $\omega = 0.3\ a_0^{-1}$ represents the standard value given in the literature, while $\omega = 0.23\ a_0^{-1}$ has been optimized by employing the procedure by Stein et al.[15] and using the standard 6-31G* Pople basis set.

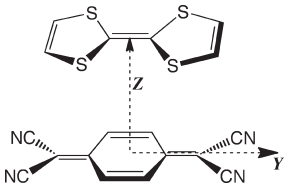

Figure 1. Tetrathiafulvalene−tetracyanoquinodimethane model complex in the cofacial geometry. The two molecular planes are parallel to one another.

In order to assess the reliability of the single-reference approaches for describing the D/A complex, complete active-space self-consistent field (CASSCF) computations and broken-symmetry unrestricted DFT computations were also performed. The active space for CASSCF computations included up to eight electrons in seven MOs. The unrestricted DFT results will not be presented, as they collapse to those obtained from the restricted DFT formalism. The interaction energies were calculated with respect to the isolated monomers and were corrected for the basis-set superposition error (BSSE) by the counterpoise correction method of Boys and Bernardi.[39] For each method, charge transfer in the ground state is computed on the basis of the natural population analysis (NPA)[40] charges.

The benchmark level considered in this work is SCS-MP2, which has been shown to reduce the overbinding of the conventional MP2 method. Given the complexity of our system and the large basis set considered here, we were not able to produce CCSD(T) values for the interaction energies. However, a comparison of CCSD(T) and SCS-MP2 computations in a smaller 6-31G* basis gives very good agreement between these approaches. Couplings between the frontier orbitals of TTF and TCNQ have been calculated according to the approach described by Valeev et al.[41] with the corresponding matrix elements evaluated with Gaussian 09.

RESULTS AND DISCUSSION

1. Frontier Orbital Analysis. On the basis of calculations on the isolated molecules, the $HOMO_{TTF}-LUMO_{TCNQ}$ energy gaps, defined as $E[LUMO_{TCNQ}] - E[HOMO_{TTF}]$, are presented in Table 1 for the various functionals and are plotted in Figure 2 along with the frontier orbital energies themselves ($HOMO_{TTF}$, $HOMO-1_{TTF}$, and $LUMO_{TCNQ}$) as a function of the percentage of HF exchange in the functional (% HF). Both the $HOMO_{TTF}$ and $HOMO-1_{TTF}$ have been included in the inset of Figure 2, as both are relevant to our discussion of the charge transfer, a point that will made more clear in the discussion below. Figure 2 shows a linear increase in the $HOMO_{TTF}-LUMO_{TCNQ}$ gap as a function of the percentage in HF exchange.

dx.doi.org/10.1021/ct1005517 |*J. Chem. Theory Comput.* 2011, 7, 602–609

Table 1. Fraction of HF Exchange, Computed $HOMO_{TTF}-LUMO_{TCNQ}$ Gaps, and Computed Ground-State Charge Transfer (both at the SCS-MP2 geometry and the minimum-energy geometry for the functional) for Cofacial and Parallel-Displaced Structures of the TTF−TCNQ Model Complex for Various Functionals

			q^{GS} (TTF)			
method	% HF	Δ(L−H)[a] (eV)	cofacial[b] (SCS-MP2)	cofacial[c] (min)	parallel-displaced[d] (SCS-MP2)	parallel-displaced[c] (min)
TPSSh	10	−0.802	0.081		0.308	
B3LYP	20	−0.324	0.066	0.019	0.285	0.199
B97-1	21	−0.260	0.071	0.050	0.281	0.234
PBE0	25	−0.051	0.058	0.042	0.260	0.233
BMK	42	0.816	0.053	0.059	0.206	0.216
BHandH	50	1.386	0.054	0.111	0.160	0.242
M06-2X	54	1.514	0.047	0.074	0.153	0.213
M05-2X	56	1.532	0.049	0.081	0.166	0.232
LRC-ωPBEh	79.9[e]	2.966	0.040	0.027	0.132	0.091
ωB97X-D	80.9[e]	3.020	0.042	0.053	0.129	0.157
ωB97X-0.23	83.4[e]	3.156	0.041		0.118	
ωB97X-0.3	92.3[e]	3.646	0.037	0.037	0.083	0.083
LC-ωPBE	97.7[e]	3.941				
M06-HF	100	4.139	0.035	0.076	0.063	0.142
HF		4.843	0.026		0.045	
CASSCF			0.034		0.039	
MP2			0.052	0.052	0.095	0.095

[a] $\Delta E(LUMO_{TCNQ}HOMO_{TTF})$ for the isolated molecules. [b] Cofacial geometry at an intermolecular separation of 3.45 Å, corresponding to the SCS-MP2 mimimum. [c] Cofacial or parallel displaced (at fixed 3.45 Å interplanar distance) geometry corresponding to the minimum-energy geometry for the functional. [d] Parallel displacement of 3.00 Å at a fixed intermolecular distance of 3.45 Å, corresponding to the SCS-MP2 minimum. [e] Effective values (see text for details).

The $HOMO-1_{TTF}-LUMO_{TCNQ}$ gap shows a nearly identical progression (as can be expected from the plots of the orbital energies in the inset).

The M06-HF functional, which contains 100% HF exchange, provides the greatest energy gap value among all DFT functionals, slightly over 4 eV. It is topped only by the HF value itself, 4.87 eV; however, as HF virtual orbitals are constructed on the basis of an $N + 1$-electron system, the HOMO−LUMO gaps from HF are expected to be overestimated. At the other extreme, the TPSSh functional (that contains just 10% HF exchange) gives a "negative" gap of −0.802 eV; along with the other low HF-exchange functionals (B3LYP, B97-1, and PBE0), it provides an unphysical picture of the frontier energy levels since the $LUMO_{TCNQ}$ energy is calculated to be lower than the $HOMO_{TTF}$ energy for the isolated molecules. Such results are an artifact of these methods, as the experimental gas-phase values for the ionization potential of TTF and the (exothermic) electron affinity of TCNQ are 6.7 eV[42] and 2.8 eV,[43] respectively (which gives an energy difference of 3.9 eV and suggests that only a partial charge transfer should be expected when the complex forms). A preliminary conclusion based on the frontier-orbital analysis is that DFT methods including a low percentage of HF exchange will be inappropriate for describing complexes such as TTF−TCNQ.

Given that a positive value for the $HOMO_{TTF}-LUMO_{TCNQ}$ gap should be expected, the functionals containing more than 40−50% HF exchange (i.e., BMK, BHandH, M05-2X, M06-2X, and M06-HF) and the ω functionals provide for at least a reasonably physical description. Comparing the $HOMO_{TTF}-LUMO_{TCNQ}$ gaps from Table 1 to the difference between the experimental IP value for TTF and the EA value for TCNQ (3.9 eV), it is found that the ωB97X-0.3, LC-ωPBE, and M06-HF functionals give reliable results.

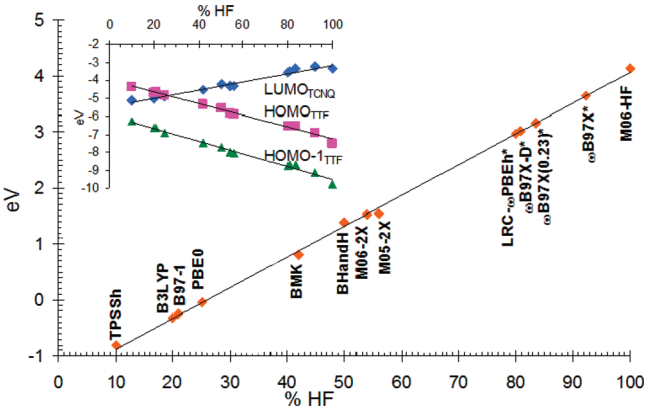

Figure 2. Computed $HOMO_{TTF}-LUMO_{TCNQ}$ gap (orange diamonds). [Inset] Computed $HOMO_{TTF}$, $HOMO-1_{TTF}$, and $LUMO_{TCNQ}$ energies as a function of the percentage of HF exchange. The % HF for ω functionals are effective values (see text for details).

With regard to the ω functionals, it is not possible to assign explicit values for the percentage of HF exchange. However, it is reasonable to expect that the ω functionals with 100% HF exchange at long range contain a greater extent of HF exchange than BHandH, M05-2X, and M06-2X functionals, but a lower extent than M06-HF, as the latter only has HF exchange. Larger ω values result in a greater amount of exact exchange (being evaluated through the second term on the rhs of eq 1). The LRC-ωPBEh and ωB97X-D functionals with $\omega = 0.2$ a_0^{-1} consequently contain a lesser degree of long-range HF exchange than

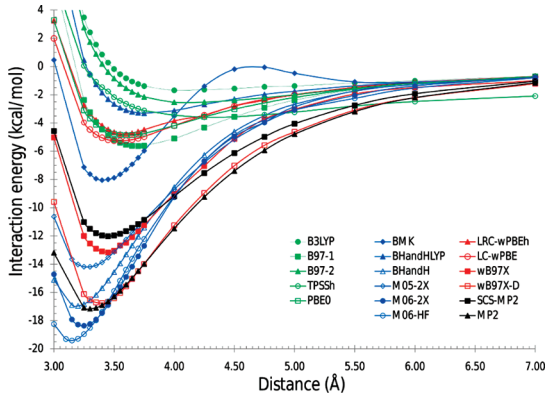

Figure 3. Potential energy surfaces for the cofacial model complex of TTF−TCNQ computed at various levels of theory with a 6-311++G** basis. All values are corrected for BSSE as described in the text.

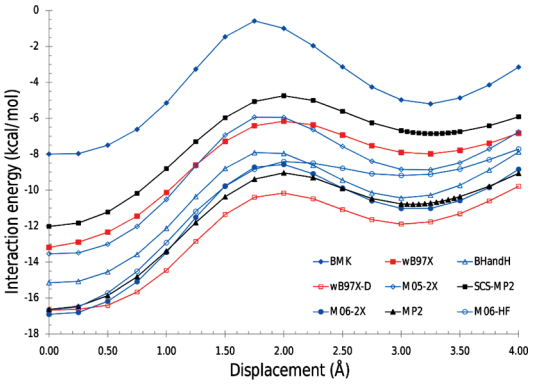

Figure 4. Potential energy surfaces for the parallel-displaced model complex of TTF−TCNQ (with a fixed interplanar separation of 3.45 Å) computed at various levels of theory and with a 6-311++G** basis. All values are corrected for BSSE as described in the text.

ωB97X-0.23 (ω = 0.23 a_0^{-1}), which in turn contains less HF exchange than ωB97X-0.3 (ω = 0.3 a_0^{-1}) or LC-ωPBE (ω = 0.4 a_0^{-1}). Using the $HOMO_{TTF}-LUMO_{TCNQ}$ gaps and the percentage of exact exchange for the standard functionals (results from Table 1), we have used a simple linear regression to approximate the relationship between the computed gaps and the percentage of exact exchange, see Figure 2. This relation has been employed to assign *effective* percentages of exact exchange to the ω functionals; the values are calculated to range between 80 and 97% (Table 1), which indicates the significance of the long-range exact exchange in these functionals. It is worth noting that, while remaining greater than ∼60% HF, these effective values could be different for other systems, as the contribution from HF exchange is a function of the electronic density.[16]

2. Interaction Energies. The ground-state charge transfer will depend heavily upon the relative geometry and orientation of the D/A molecules in the complex, falling off quickly with distance (due to the exponential decay of the overlap) and being impacted strongly by symmetry considerations (as discussed below). We thus turn our attention to the description of the ground-state potential energy surfaces. The potential energy surfaces provided by several functionals for the cofacial structure can be found in Figure 3. The SCS-MP2 values (taken here as a reference) predict a minimum of 12.02 kcal mol^{-1} (as compared to 17.16 kcal mol^{-1} at the MP2 level) at a separation of 3.45 Å between the molecular planes (3.25 Å at the MP2 level). The MP2 approach thus appears to substantially overbind for this system. As mentioned previously, CCSD(T) and SCS-MP2 computations in the smaller 6-31G* basis predict similar binding energies (7.24 and 8.16 kcal mol^{-1}, respectively), which are much smaller than the MP2 reults for this basis set (11.75 kcal mol^{-1}).

Turning to the results for the DFT approaches collected in Figure 3, a rough separation into two groups of functionals can be observed. In general, only the long-range corrected functionals (in red) and functionals containing a high admixture of exact HF exchange (in blue) provide potential energy surfaces and interaction energies in overall good semiquantitative or qualitative agreement with the SCS-MP2 results. The best performance is shown by the ωB97X functional (whose results differ from the SCS-MP2 results by ∼1 kcal mol^{-1}), while the M05-2X, BHandH, ωB97X-D, M06-2X, and M06-HF functionals overestimate the interaction energy by ∼2−7 kcal mol^{-1}. The spurious maximum observed with the BMK functional (which remains even with an unrestricted approach) is surprising. On the other hand, all of the traditional functionals containing less than ∼30% HF exchange (in green) provide an overall very poor description of the interaction energies with respect to the benchmark results, underbinding by more than ∼7 kcal mol^{-1}.

While there are many differences between the two groups of functionals, we will focus here on the correlation with the amount of exact exchange in the functionals (see also Table 1). It is well-known that the inclusion of exact exchange is important for correcting the self-interaction error effects, which in turn reduces the delocalization error.[11b] Accordingly, the standard hybrid functionals containing a small fraction of HF exchange (such as TPSSh, B3LYP, and PBE0) show an overall poor description of the binding. While high admixtures of exact exchange appear to be required for the description of the binding in the TTF−TCNQ model complex, the differences between, for instance, the BHandH and BHandHLYP results (both containing 50% HF exchange) indicate the importance of the specific form of the exchange functional as well. Similar observations can be made for the ω functionals. The ωB97X functional (containing up to 100% exact exchange at long range) provides the best performance, which underlines the importance of the long-range exact exchange. However, ωB97X-D (containing also up to 100% exact exchange at long range) overestimates the interaction energy, while LRC-ωPBEh and LC-ωPBE underestimate by more than 7 kcal mol^{-1} in comparison to SCS-MP2. These observations point clearly to the importance of a careful balance between the long-range exact exchange and the quality of the short-range exchange and correlation.

It is worth mentioning that the ω values in the considered LR-corrected functionals vary between 0.2 and 0.4 a_0^{-1}; this corresponds to approximately $1/\omega \sim 3-5$ a_0 and indicates that the separation between the short-range and long-range regions is located around 2−3 Å. The TTF−TCNQ intermolecular separation lies just beyond this range (3.45 Å); as a consequence, the complex appears to be qualitatively correctly described by both middle-range functionals (M06-2X and M05-2X) as well as long-range corrected functionals.

The potential energy surfaces for the parallel-displaced configurations (at a fixed intermolecular distance of 3.45 Å) are included in Figure 4 for MP2, SCS-MP2, and a subset of the DFT functionals investigated. A local minimum (some 5 kcal mol^{-1} above the cofacial configuration) is predicted by all approaches for a parallel displacement around 3.25 Å. Geometry optimizations

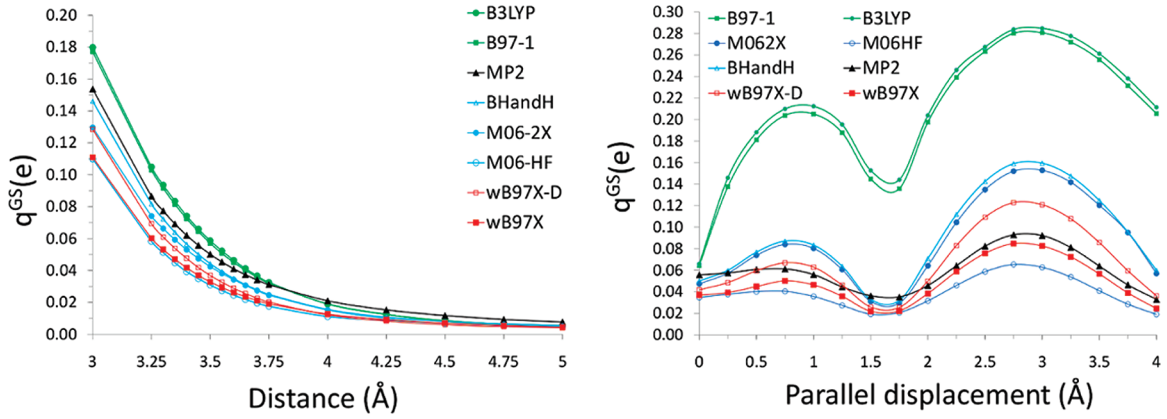

Figure 5. NPA charge transferred in the ground state (q^{GS}) calculated with the different functionals, plotted either as a function of (left panel) the interplanar distance in the cofacial configuration or (right panel) the horizontal displacement at a fixed interplanar distance of 3.45 Å for the TTF−TCNQ model system.

starting from these points give real minima without imaginary frequencies; the calculated interaction energies on the order of 7−12 kcal mol^{-1} are consistent with the presence of complexes with such configurations in polar solvents, as observed experimentally by Tomkiewicz et al.[44]

The overall performance of ωB97X remains quite good for the description of the parallel-displaced structure, where the results can be seen to strongly parallel the SCS-MP2 results. For the case of the Minnesota functionals, M05-2X provides interaction energies that are overall closer to the SCS-MP2 results. Both M05-2X and M06-2X (each containing slightly more than 50% HF exchange) predict a slightly deeper well for the second minimum (at a parallel displacement of approximately 3.0 Å), while M06-HF predicts a much shallower second minimum. All of the functionals presented contain a high admixture of HF exchange and provide a qualitatively correct description of the parallel-displaced potential energy surface.

3. Ground-State Charge Transfer. In D/A systems, the ground-state wave function (Ψ^{GS}) can be expressed as a linear combination of the neutral donor and acceptor components ($\Psi^{D,A}$) with a small admixture of a charge-transfer state (Ψ^{CT}):

$$\Psi^{GS} = \Psi^{D,A} + c\Psi^{CT} \quad (2)$$

The mixing of $\Psi^{D,A}$ and Ψ^{CT} in this expression is proportional to the coupling (V) between the covalent and ionic states and inversely proportional to their energy difference (ΔE). When the wave function in eq 2 is taken as a first-order corrected wave function in a perturbative development, the coefficient describing the contribution of the charge-transfer state is given by $c = V/\Delta E$, and the amount of charge transferred in the ground state can be expressed as[17a] $q \propto (V/\Delta E)^2$. Thus, in the framework of a monodeterminantal description of the ground-state wave function where the charge transfer can be considered as an electron jump from an occupied frontier orbital (HOMO or HOMO−1) of TTF to the LUMO of TCNQ, the energy difference between these orbitals as well as their electronic coupling are the key parameters defining the amount of charge transferred.

The electronic coupling between the orbitals is very sensitive to the relative orientations/positions of the molecules forming the complex[45] and dominates the evolution of charge transfer with increasing intermolecular distance due to the exponential decrease in wave function overlap. This can be seen when examing the left panel of Figure 5, where q^{GS} is depicted as a function of intermolecular distance in the cofacial configuration. The amount of charge transferred clearly falls off quickly with increasing separation (decreasing coupling) between the TTF and TCNQ molecules. While all functionals depict this feature, the functionals containing small amounts of HF exchange (B3LYP and B97−1) provide q^{GS} values that fall off more quickly in the intermediate region than for MP2 or the LRC and meta-GGA functionals.

The dependence of q^{GS} on intermolecular separation can also be clearly observed from the results in Table 1. At the SCS-MP2 minimum (3.45 Å), both B3LYP and B97-1 functionals (that contain similar percentages of HF exchange) provide similar descriptions of q^{GS} in the cofacial arrangement and values somewhat larger than for BHandH. However, when comparing the minimum-energy cofacial structures for each functional, the much poorer performance of B3LYP and BHandH in describing the intermolecular separation manifests in a rather poor description of q^{GS} as well. B3LYP predicts a much larger intermolecular separation (see Figure 3) and consequently a much smaller q^{GS}, while BHandH strongly overbinds and presents a very short intermolecular distance and thus a greatly exaggerated q^{GS} value. The overall more reasonable description of the PES afforded by B97-1 provides for q^{GS} values (at the respective minima) that are very close to the SCS-MP2 values.

With respect to the electronic coupling, the significance of the wave function overlap is clearly delineated when comparing the cofacial and parallel-displaced conformations of the TTF−TCNQ complex. The $HOMO_{TTF}$, $HOMO-1_{TTF}$, and $LUMO_{TCNQ}$ orbitals (depicted in Figure 6) are all relevant for understanding the ground-state charge transfer in TTF−TCNQ. Both the $HOMO-1_{TTF}$ and $LUMO_{TCNQ}$ orbitals possess *ungerade* symmetry, while the $HOMO_{TTF}$ is of *gerade* symmetry. In the cofacial conformation, the wave function overlap (and thus the electronic coupling) between $HOMO_{TTF}$ and $LUMO_{TCNQ}$ vanishes for symmetry reasons, leaving the $HOMO-1_{TTF}$−$LUMO_{TCNQ}$ coupling (and energy difference) as the leading contributor to the charge transfer.

This effect can also be observed from the q^{GS} values depicted for the parallel-displaced configuration in Figure 5 (right panel). For a given parallel-displaced geometry, the $HOMO_{TTF}$−$LUMO_{TCNQ}$ overlap (and the corresponding electronic coupling) depends on the relative positions of the $HOMO_{TTF}$ and $LUMO_{TCNQ}$ nodal surfaces (Figure 6). The minimum observed

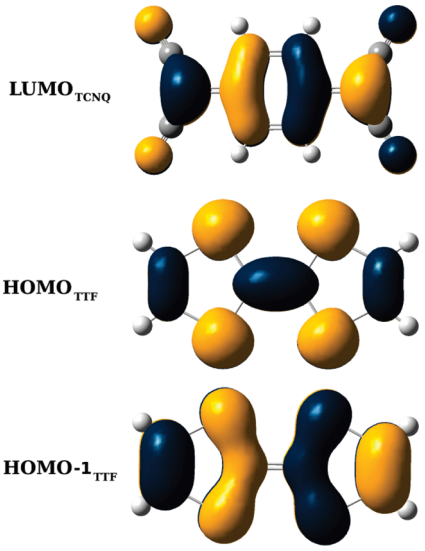

Figure 6. Sketch of the HOMO-1_{TTF}, HOMO$_{TTF}$, and LUMO$_{TCNQ}$ orbitals.

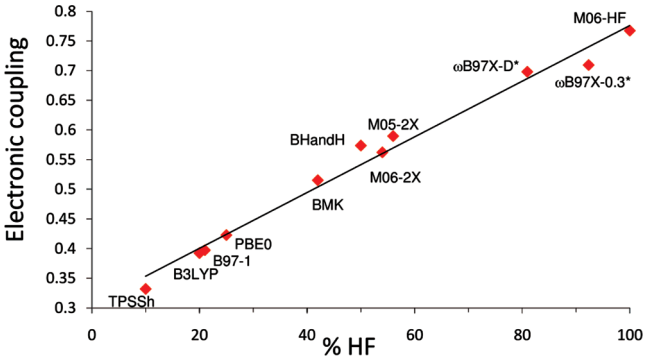

Figure 7. Electronic coupling (eV) between HOMO-1_{TTF} and LUMO$_{TCNQ}$ for the cofacial TTF−TCNQ model system (3.45 Å intermolecular distance) calculated with various functionals and plotted as a function of % HF exchange.

in the q^{GS} values for parallel displacements around 1.75 Å and the maximum observed for displacements of *ca.* 3.0 Å are consistent with the HOMO$_{TTF}$−LUMO$_{TCNQ}$ couplings of 0.075 and 0.708 eV calculated at these geometries, respectively (absolute values calculated with the ωB97X functional). The decrease in the q^{GS} values with parallel displacements around 1.5−1.75 Å is driven by a decreased HOMO-1_{TTF}−LUMO$_{TCNQ}$ coupling and a mere increase in the HOMO$_{TTF}$−LUMO$_{TCNQ}$ coupling (which can be ascribed to the small HOMO$_{TTF}$−LUMO$_{TCNQ}$ overlap value of 0.0057 at 1.75 Å). The importance of employing functionals with a high admixture of HF exchange can be seen when considering the q^{GS} values for the parallel-displaced structures in the right panel of Figure 5, where both B3LYP and B97-1 greatly overestimate the contribution from the HOMO$_{TTF}$−LUMO$_{TCNQ}$ coupling and, as a result, the amount of charge transferred.

Thus, changes in geometry and conformation do strongly impact the electronic coupling and charge transfer; also, simple symmetry arguments can explain vanishingly small charge-transfer values. However, for a given geometry, the electronic coupling can still vary largely as a function of the choice of DFT functional. This is demonstrated to be the case for the cofacial geometry, see

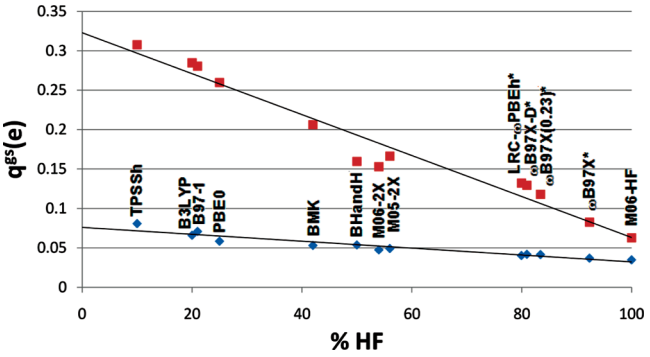

Figure 8. NPA charge transferred in the ground state (q^{GS}) calculated with the different functionals, plotted as a function of the HF exchange for the cofacial (blue) and parallel-displaced (red) configurations of the TTF−TCNQ model complex at a fixed intermolecular distance of 3.45 Å.

Figure 7, where the electronic coupling between HOMO-1_{TTF} and LUMO$_{TCNQ}$ is calculated to vary by a factor of 2 among the various functionals. The computed couplings follow a nearly linear dependence upon the amount of exchange, increasing by a factor of ∼2.3 on going from the TPSSh functional (10% HF) to the M06-HF functional (100% HF).

The NPA charges in the ground state (q^{GS}) for both the cofacial configuration and the parallel-displaced configuration of 3.0 Å are included in Table 1 and plotted in Figure 8. The MP2 calculations, which are generally used for the evaluation of net atomic or fragment charges, give values that are between those from HF and TPSSh. For the cofacial geometry at an intermolecular distance of 3.45 Å (absolute minimum in the potential energy surface), the ground-state charge transfer varies by only 0.05*e* among the functionals with a maximum value of 0.08*e* for TPSSh. As underlined above, the small values calculated in the case of the cofacial geometry are a consequence of the symmetries of the HOMO$_{TTF}$ and LUMO$_{TCNQ}$ orbitals (Figure 6), which leads to a vanishing electronic coupling; on the other hand, in spite of the rather strong coupling between HOMO-1_{TTF} and LUMO$_{TCNQ}$, there exists a substantial energetic difference between these orbitals (roughly 2 eV larger than the HOMO−LUMO gap, Figure 2).

This situation is very different in the parallel-displaced configuration where the amount of charge transferred increases in some instances to over 0.3*e*, see Figure 8. It is interesting to note that, while the coupling increases (in some cases by more than a factor of 2), the amount of charge transferred decreases almost linearly with the admixture of exchange. Recalling that $q \propto (V/\Delta E)^2$, it can be readily understood that the dominant factor is the large (∼5 eV) increase in the HOMO$_{TTF}$−LUMO$_{TCNQ}$ (HOMO-1_{TTF}−LUMO$_{TCNQ}$) energy splitting in the denominator with increased % HF.

4. Reliability of DFT Charge-Transfer Values. In order to assess the reliability of the results obtained in the framework of the monodeterminantal approach, CASSCF computations were performed for both cofacial and parallel-displaced (corresponding to the greater q^{GS}) geometries. The active space employed includes eight electrons in seven molecular orbitals, although the HOMO$_{TTF}$, HOMO-1_{TTF}, and LUMO$_{TCNQ}$ orbitals provide the dominant contributions to the charge transfer. In both geometries, the calculated CASSCF NPA charges (Table 1) are lower than 0.1*e* and the coefficients for the charge-transfer configurations in the CASSCF wave function are vanishingly

dx.doi.org/10.1021/ct1005517 |*J. Chem. Theory Comput.* 2011, 7, 602–609

small. Thus, the wave function for the complex is strongly dominated by the closed-shell electronic configuration (and not the open-shell singlet configuration that would be expected in the limit of full transfer of an electron). Therefore, single-reference approaches such as those employed here should provide a reliable description of the system. These results underline that a small partial charge transfer should be expected in the TTF−TCNQ complex, which appears to be consistent with the experimental observation[44] that only a limited amount (∼5%) of TCNQ anions is detected in a TTF−TCNQ mixture in solution in a highly polar solvent such as acetonitrile (dielectric constant of 36.64) as well as with the values computed from DFT functionals with a high degree of HF exchange.

With regard to the DFT approaches, the electronic coupling values presented in Figure 7 (which vary between ∼0.3 and 0.8 eV) demonstrate the relatively strong character of the electronic coupling in this system. By analogy with the single molecule electron transport measurements[18] and theoretical results,[19] the amount of charge transferred in this case is expected to vary continuously with the HOMO−LUMO gap, which means that the mono- and multideterminantal methods should give qualitatively similar descriptions. However, the poor description of the HOMO−LUMO gap provided by functionals containing only a small percentage of HF exchange (i.e., TPSSh, B97-1, B3LYP, and PBE0) results in an overestimation of the q^{GS} values. On the other hand, the functionals containing more than 50%HF exchange (i.e., BHandH, M052X, M062X, M06HF, and the ω functionals) give q^{GS} values lower than 0.2*e*; this is in qualitative agreement with the CASSCF calculations (reported by Avilov et al.[17a] and in this study) but also with the experimental observations.[44,46] However, when considering the minimum-energy geometries (Table 1, last column), the meta-GGA functionals are found to provide q^{GS} values that are slightly greater than 0.2*e* and in lesser agreement with the MP2 value of 0.095*e*, while the best agreement is found for the LRC-ωPBEh and ωB97X functionals. Again, the functionals containing a low %HF exchange overestimate the q^{GS} values.

We note that the CASSCF q^{GS} values shown in Table 1 are similar to those from HF, indicating the need for dynamical electron correlation missing from both the HF and CASSCF treatments. Thus, when considering the MP2 value of 0.095*e* (which is generally considered here as a benchmark level), it can be concluded that the ωB97X functional provides reliable results for both ω values. This is also consistent with the comparison made above between the computed HOMO−LUMO gaps and the ∼3.9 eV experimental difference between IP(TTF) and EA(TCNQ), for which the ωB97X functional also provides very good agreement.

CONCLUSIONS

DFT calculations with a number of functionals have been carried out on a TTF−TCNQ model complex in order to evaluate their description of ground-state charge transfer. We have assessed the performance of the functionals for describing quantities such as the $HOMO_{TTF}$−$LUMO_{TCNQ}$ energy difference, the binding energy in the ground state, the strength of the electronic coupling between frontier molecular orbitals, and the extent of charge transfer in the ground state.

The inclusion of large amounts (more than 60%) of long-range HF exchange in the functionals seems to be crucial in order to obtain reliable results for all quantities. Among the functionals considered in this study, the long-range corrected functional ωB97X is found to give reliable results for the ensemble of the calculated properties. Standard hybrid functionals containing only a small percentage of HF exchange are found to be inadequate for properties directly related to the $HOMO_{TTF}$−$LUMO_{TCNQ}$ energy gap.

For a fixed geometry, a linear relationship is observed between the degree of charge transfer, the $HOMO_{TTF}$−$LUMO_{TCNQ}$ gap, and the percentage of HF exchange. Both the electronic coupling and the amount of charge transferred are shown to vary largely among the various functionals as well as with changes in the relative positions of the molecules. This highlights the importance of choosing a method capable of describing the potential energy surface as well as the relevant electronic couplings. The role of exchange in the evaluation of electronic couplings is the focus of ongoing work in our group.

AUTHOR INFORMATION

Corresponding Author

*E-mail: jean-luc.bredas@chemistry.gatech.edu.

Notes

[†]On leave from Laboratoire de Physicochimie des Polymères et des Interfaces (LPPI), Université de Cergy-Pontoise, 5 mail Gay-Lussac, F-95031 Cergy-Pontoise Cedex, France.

ACKNOWLEDGMENT

This work has been supported by the Center for Advanced Molecular Photovoltaics, Award No. KUS-C1-015-21, made by King Abdullah University of Science and Technology (KAUST); the Georgia Research Alliance; the STC Program of the National Science Foundation under Award DMR-0120967; and the University of Cergy-Pontoise, France.

REFERENCES

(1) (a) Mulliken, R. S. *J. Phys. Chem.* **1952**, *56*, 801–822. (b) Mulliken, R. S. *J. Chim. Phys., Chim. Biol.* **1964**, *61*, 20–38. (c) Mulliken, R. S.; Person, W. B. *Annu. Rev. Phys. Chem.* **1962**, *13*, 107–126. (d) Orgel, L. E.; Mulliken, R. S. *J. Am. Chem. Soc.* **1957**, *79*, 4839–4846.

(2) (a) Kippelen, B.; Bredas, J. L. *Energy Environ. Sci.* **2009**, *2*, 251–261. (b) Bredas, J. L.; Norton, J. E.; Cornil, J.; Coropceanu, V. *Acc. Chem. Res.* **2009**, *42*, 1691–1699.

(3) Walzer, K.; Maennig, B.; Pfeiffer, M.; Leo, K. *Chem. Rev.* **2007**, *107*, 1233–1271.

(4) Koster, L. J. A.; Smits, E. C. P.; Mihailetchi, V. D.; Blom, P. W. M. *Phys. Rev. B* **2005**, 72.

(5) (a) Potscavage, W. J.; Sharma, A.; Kippelen, B. *Acc. Chem. Res.* **2009**, *42*, 1758–1767. (b) Potscavage, W. J.; Yoo, S.; Kippelen, B. *Appl. Phys. Lett.* **2008**, *93*, 193308. (c) Rand, B. P.; Burk, D. P.; Forrest, S. R. *Phys. Rev. B* **2007**, *75*, 115327. (d) Waldauf, C.; Scharber, M. C.; Schilinsky, P.; Hauch, J. A.; Brabec, C. J. *J. Appl. Phys.* **2006**, *99*, 104503.

(6) Qi, Y. B.; Sajoto, T.; Barlow, S.; Kim, E. G.; Bredas, J. L.; Marder, S. R.; Kahn, A., *J. Am. Chem. Soc.* **2009**, *131*, 12530.

(7) (a) Hamel, S.; Duffy, P.; Casida, M. E.; Salahub, D. R. *J. Electron Spectrosc. Relat. Phenom.* **2002**, *123*, 345–363. (b) Shankar, R.; Senthilkumar, K.; Kolandaivel, P. *Int. J. Quantum Chem.* **2009**, *109*, 764–771. (c) Zhang, G.; Musgrave, C. B. *J. Phys. Chem. A* **2007**, *111*, 1554–1561.

(8) (a) Hua, X. L.; Chen, X. J.; Goddard, W. A. *Phys. Rev. B* **1997**, *55*, 16103–16109. (b) Manby, F. R.; Knowles, P. J. *J. Chem. Phys.* **2000**, *112*, 7002–7007.

(9) Perdew, J. P.; Zunger, A. *Phys. Rev. B* **1981**, *23*, 5048–5079.

(10) (a) Ruzsinszky, A.; Perdew, J. P.; Csonka, G. I.; Vydrov, O. A.; Scuseria, G. E. *J. Chem. Phys.* **2007**, *126*. (b) Braida, B.; Hiberty, P. C.;

Savin, A. *J. Phys. Chem. A* **1998**, *102*, 7872–7877. (c) Bally, T.; Sastry, G. N. *J. Phys. Chem. A* **1997**, *101*, 7923–7925.
(11) (a) Kummel, S.; Kronik, L.; Perdew, J. P. *Phys. Rev. Lett.* **2004**, *93*. (b) Mori-Sanchez, P.; Wu, Q.; Yang, W. T. *J. Chem. Phys.* **2003**, *119*, 11001–11004. (c) van Gisbergen, S. J. A.; Schipper, P. R. T.; Gritsenko, O. V.; Baerends, E. J.; Snijders, J. G.; Champagne, B.; Kirtman, B. *Phys. Rev. Lett.* **1999**, *83*, 694–697.
(12) (a) Dreuw, A.; Head-Gordon, M. *J. Am. Chem. Soc.* **2004**, *126*, 4007–4016. (b) Dreuw, A.; Weisman, J. L.; Head-Gordon, M. *J. Chem. Phys.* **2003**, *119*, 2943–2946.
(13) Becke, A. D. *J. Chem. Phys.* **1993**, *98*, 5648–5652.
(14) (a) Kamiya, M.; Tsuneda, T.; Hirao, K. *J. Chem. Phys.* **2002**, *117*, 6010–6015. (b) Adamson, R. D.; Dombroski, J. P.; Gill, P. M. W. *J. Comput. Chem.* **1999**, *20*, 921–927. (c) Leininger, T.; Stoll, H.; Werner, H. J.; Savin, A. *Chem. Phys. Lett.* **1997**, *275*, 151–160.
(15) Stein, T.; Kronik, L.; Baer, R. *J. Am. Chem. Soc.* **2009**, *131*, 2818.
(16) Baer, R.; Neuhauser, D. *Phys. Rev. Lett.* **2005**, *94*, 043002.
(17) (a) Avilov, I.; Geskin, V.; Cornil, J. *Adv. Funct. Mater.* **2009**, *19*, 624–633. (b) Geskin, V.; Stadler, R.; Cornil, J. *Phys. Rev. B* **2009**, *80*, 085411.
(18) Danilov, A.; Kubatkin, S.; Kafanov, S.; Hedegard, P.; Stuhr-Hansen, N.; Moth-Poulsen, K.; Bjornholm, T. *Nano Lett.* **2008**, *8*, 1–5.
(19) Toher, C.; Filippetti, A.; Sanvito, S.; Burke, K. *Phys. Rev. Lett.* **2005**, *95*, 146402.
(20) Lee, C. T.; Yang, W. T.; Parr, R. G. *Phys. Rev. B* **1988**, *37*, 785–789.
(21) Tao, J. M.; Perdew, J. P.; Staroverov, V. N.; Scuseria, G. E. *Phys. Rev. Lett.* **2003**, *91*, 146401.
(22) Hamprecht, F. A.; Cohen, A. J.; Tozer, D. J.; Handy, N. C. *J. Chem. Phys.* **1998**, *109*, 6264–6271.
(23) Wilson, P. J.; Bradley, T. J.; Tozer, D. J. *J. Chem. Phys.* **2001**, *115*, 9233–9242.
(24) (a) Ernzerhof, M.; Scuseria, G. E. *J. Chem. Phys.* **1999**, *110*, 5029–5036. (b) Adamo, C.; Barone, V. *J. Chem. Phys.* **1999**, *110*, 6158–6170.
(25) Boese, A. D.; Martin, J. M. L. *J. Chem. Phys.* **2004**, *121*, 3405–3416.
(26) As implemeted in Gaussian 09.
(27) As implemeted in Gaussian 09.
(28) Zhao, Y.; Schultz, N. E.; Truhlar, D. G. *J. Chem. Theory Comput.* **2006**, *2*, 364–382.
(29) Zhao, Y.; Truhlar, D. G. *Acc. Chem. Res.* **2008**, *41*, 157–167.
(30) Chai, J. D.; Head-Gordon, M. *J. Chem. Phys.* **2008**, *128*, 084106.
(31) Chai, J. D.; Head-Gordon, M. *Phys. Chem. Chem. Phys.* **2008**, *10*, 6615–6620.
(32) Rohrdanz, M. A.; Martins, K. M.; Herbert, J. M. *J. Chem. Phys.* **2009**, *130*, 054112.
(33) (a) Vydrov, O. A.; Heyd, J.; Krukau, A. V.; Scuseria, G. E. *J. Chem. Phys.* **2006**, *125*, 074106. (b) Vydrov, O. A.; Scuseria, G. E. *J. Chem. Phys.* **2006**, *125*, 234109.
(34) Frisch, M. J.; Trucks, G. W.; Schlegel, H. B. *Gaussian 09*, revision A.1; Gaussian, Inc.: Pittsburgh, PA, 2009.
(35) Kong, J.; White, C. A.; Krylov, A. I.; Sherrill, D.; Adamson, R. D.; Furlani, T. R.; Lee, M. S.; Lee, A. M.; Gwaltney, S. R.; Adams, T. R.; Ochsenfeld, C.; Gilbert, A. T. B.; Kedziora, G. S.; Rassolov, V. A.; Maurice, D. R.; Nair, N.; Shao, Y. H.; Besley, N. A.; Maslen, P. E.; Dombroski, J. P.; Daschel, H.; Zhang, W. M.; Korambath, P. P.; Baker, J.; Byrd, E. F. C.; Van Voorhis, T.; Oumi, M.; Hirata, S.; Hsu, C. P.; Ishikawa, N.; Florian, J.; Warshel, A.; Johnson, B. G.; Gill, P. M. W.; Head-Gordon, M.; Pople, J. A. *J. Comput. Chem.* **2000**, *21*, 1532–1548.
(36) Werner, H.-J.; Knowles, P. J.; Lindh, R.; Manby, F. R.; Schütz, M.; Celani, P.; Korona, T.; Mitrushenkov, A.; Rauhut, G.; Adler, T. B.; Amos, R. D.; Bernhardsson, A.; Berning, A.; Cooper, D. L.; Deegan, M. J. O.; Dobbyn, A. J.; Eckert, F.; Goll, E.; Hampel, C.; Hetzer, G.; Hrenar, T.; Knizia, G.; Köppl, C.; Liu, Y.; Lloyd, A. W.; Mata, R. A.; May, A. J.; McNicholas, S. J.; Meyer, W.; Mura, M. E.; Nicklass, A.; Palmieri, P.; Pflüger, K.; Pitzer, R.; Reiher, M.; Schumann, U.; Stoll, H.; Stone, A. J.; Tarroni, R.; Thorsteinsson, T.; Wang, M.; Wolf, A. *MOLPRO*, version 2009.1; University College Cardiff Consultants Limited: Cardiff, U. K., 2009.
(37) Moller, C.; Plesset, M. S. *Phys. Rev.* **1934**, *46*, 0618–0622.
(38) Grimme, S. *J. Chem. Phys.* **2003**, *118*, 9095–9102.
(39) Boys, S. F.; Bernardi, F. *Mol. Phys.* **1970**, *19*, 553.
(40) Reed, A. E.; Weinstock, R. B.; Weinhold, F. *J. Chem. Phys.* **1985**, *83*, 735–746.
(41) Valeev, E. F.; Coropceanu, V.; da Silva, D. A.; Salman, S.; Bredas, J. L. *J. Am. Chem. Soc.* **2006**, *128*, 9882–9886.
(42) Lichtenberger, D. L.; Johnston, R. L.; Hinkelmann, K.; Suzuki, T.; Wudl, F. *J. Am. Chem. Soc.* **1990**, *112*, 3302–3307.
(43) Compton, R. N.; Cooper, C. D. *J. Chem. Phys.* **1977**, *66*, 4325–4329.
(44) Tomkiewi., Y; Torrance, J. B.; Scott, B. A.; Green, D. C. *J. Chem. Phys.* **1974**, *60*, 5111–5112.
(45) Bredas, J. L.; Calbert, J. P.; da Silva, D. A.; Cornil, J. *Proc. Natl. Acad. Sci. U. S. A.* **2002**, *99*, 5804–5809.
(46) (a) Yuge, R.; Miyazaki, A.; Enoki, T.; Tamada, K.; Nakamura, F.; Hara, M. *J. Phys. Chem. B* **2002**, *106*, 6894–6901. (b) Liao, J. Y.; Ho, K. C. *Sens. Actuators, B,* **2008**, *130*, 343–350.